Deregulation of MADS-box transcription factor genes in a mutant defective in the *WUSCHEL-LIKE HOMEOBOX* gene *EVERGREEN* of *Petunia hybrida*

M. Schorderet[a], R. R. Duvvuru Muni [a,c], A. Fiebig [b], and Didier Reinhardt [a]

[a]Dept. of Biology, University of Fribourg, Fribourg, Switzerland; [b]Research Group Bioinformatics and Information Technology, Department Breeding Research, Leibniz Institute of Plant Genetics and CropPlant Research (IPK) Gatersleben, Seeland, Germany; [c]Monsanto Holdings Private Limited, Mfar Manyata Tech Park, Nagavara, Bangalore, India

ABSTRACT

Angiosperm inflorescences develop in two fundamentally different ways. In monopodial plants, for example in *Arabidopsis thaliana*, the flowers are initiated as lateral appendages of a central indeterminate inflorescence meristem. In sympodial plants, flowers arise by terminal differentiation of the inflorescence meristem, while further inflorescence development proceeds from new sympodial meristems that are generated at the flank of the terminal flower. We have used the sympodial model species *Petunia hybrida* to investigate inflorescence development. Here, we describe a mutant, *bonsai* (*bns*), which is defective in flower formation, inflorescence branching, and control of meristem size. Detailed microscopic analysis revealed that *bns* meristems retain vegetative charateristics including spiral phyllotaxis. Consistent with a block in flower formation, *bns* mutants exhibit a deregulated expression of various MADS-box genes. Molecular analysis revealed that the *bns* mutant carries a transposon insertion in the previously described *EVERGREEN* (*EVG*) gene, which belongs to the *WUSCHEL-LIKE HOMEOBOX* (*WOX*) transcription factor gene family. *EVG* falls in the *WOX9* subfamily, which has diverse developmental functions in angiosperms. The comparison of *WOX9* orthologues in five model species for flowering shows that these genes play functionally divergent roles in monopodial and sympodial plants, indicating that the *WOX9* regulatory node may have played an important role in the evolution of shoot architecture.

Introduction

After embryogenesis, plants maintain the capacity to form new organs such as leaves and floral organs (sepals, petals, stamen, carpels). This remarkable organogenetic capacity requires the maintenance of cell pools with embryogenic potential, the meristems. Meristems are tightly controlled organs that consist of undifferentiated cells including a small group of stem cells in the center. To ensure continuous organogenetic capacity, meristems can remain active for many years, for example in trees. At the onset of flowering, the vegetative apical shoot meristem is transformed into an inflorescence meristem (IM), which can acquire two fates: It can either continue to function as the main inflorescence meristem that produces flowers as lateral appendages, or it can become transformed into a flower meristem (FM), which becomes entirely consumed into a terminal flower, while a new IM is initiated at its flank. The first mode of development is referred to as a monopodial inflorescence branching and results in the formation of a raceme, the typical form of the inflorescence in many flowering plants including the model species *Arabidopsis thaliana* and *Antirrhinum majus* (snapdragon).[1] The second mode of inflorescence development is known as sympodial, and produces cymes, which are characteristic for the Solanaceae.[2–4] Sympodial development is reiterative, i.e. each newly initiated IM becomes consumed again in a terminal flower after the production of a characteristic number or organs (leaves or bracts). The structures produced during such a sympodial cycle are defined as a sympodial unit.[4]

The IM of a monopodial inflorescence retains its meristematic potential throughout inflorescence development, hence it is indeterminate, whereas the IM of a sympodial inflorescence has an inherently determinate fate.[4] A sympodial unit can comprise several leaves, like in the shoot of tomato, or it can be very short with the formation of only a new inflorescence meristem and the termination in a flower like in the tomato inflorescence meristem.[1,4] Variation of sympodial development in the Solanaceae has given rise to a tremendous diversity of inflorescence architectures.[3] Sympodial inflorescences can differ considerably, depending on the composition of the individual sympodial units, their number, and their arrangement.[1,2,4]

The IMs of monopodial plants retain a nearly constant morphology over long periods of development.[5,6] This indicates that meristem size and structure are under tight genetic control. Mutants such as the *clavata* (*clv*) mutants in *Arabidopsis*, or the *fasciated ear* mutants in maize exhibit increasing meristem size during postembryonic development, but meristem identity and transition to flowering is not affected by these mutations.[5,6] At the other end of the scale, the *wuschel* mutants lose their meristems

due to a lack of stem cell maintenance and regeneration.[7] The *CLAVATA* genes (*CLV1, CLV2*, and *CLV3*) together with *WUS* constitute a regulatory feedback mechanism that ensures constant meristem size and maintenance of an active stem cell pool in *Arabidopsis*.[8,9] Whether a similar mechanism operates in sympodial plants is unknown, however, the WUS gene and its function in stem cell maintenance are clearly conserved among angiosperms, including the Solanaceae.[10]

The inflorescence of petunia (*Petunia hybrida*) is one of the best-studied examples of sympodial development,[2,11] due to the excellent molecular-genetic tools in this model species.[12] At the onset of flowering, the apical meristem is transformed into the first flower, while a lateral portion of it gives rise to a new IM. The IM then forms two leafy bracts before it generates a new IM (in the axil of the second bract) and terminates with the formation of the second flower. This sympodial branching pattern is perpetuated many times, giving rise to the characteristic zigzag-shaped petunia inflorescence.[2]

Here, we describe a petunia mutant that is defective in the transition to flowering and in the development of normal sympodial architecture. Due to its extensive branching phenotype, it has been termed *bonsai* (*bns*). The defect in the transition to flowering is earlier than in the flower identity mutant *aberrant leaf and flower* (*alf*), in which the characteristic meristem splitting pattern is retained.[13] In contrast, *bns* mutant meristems retain mostly vegetative characteristics with the formation of leaves in spiral phyllotaxis. In agreement with this notion, transcript profiling showed that the meristems of *bns* mutants fail to induce genes involved in the transition to flowering and in flower organ identity. On the other hand, *bns* mutants have a large number of upregulated genes compared to wild type floral apices, a phenomenon that might be related to their increased meristem size. *Bns* mutants have a *dTPh1* transposon insertion in the *EVERGREEN* gene that encodes a WUSCHEL-LIKE HOMEOBOX (WOX) transcription factor in the WOX9 subfamily. Comparison of the function of *EVG* with the function of its orthologues in the monopodial model species *Arabidopsis thaliana* and *Antirrhinum majus*, in the sympodial species tomato (*Solanum lycopersicum*), and in pea (*Pisum sativum*), which forms multiple compound inflorescences, suggests that *WOX9* function represent an important regulatory node that has contributed to the evolution of the diverse inflorescence branching patterns in the Solanaceae.

Results

Isolation of the bonsai (bns) *mutant defective in flowering*

In a forward mutant screen on the *Petunia hybrida* line W138 that carries multiple copies of the transposable element *dTPh1*,[14] a mutant was isolated that is defective in flowering (Figure 1A). Although the mutant plants started bolting at the same time as the wildtype siblings, they produced only bract-like leaves in large numbers (Figure 1A). Instead of the typical zigzag inflorescence (Figure 1B,D), the mutant branched excessively resulting in a structure that resembled a small tree (Figure 1C,E), hence, it was named *bonsai* (*bns*). The bolting shoot and the bract-like organs indicate that the initial signal for the onset of flowering is produced and perceived,
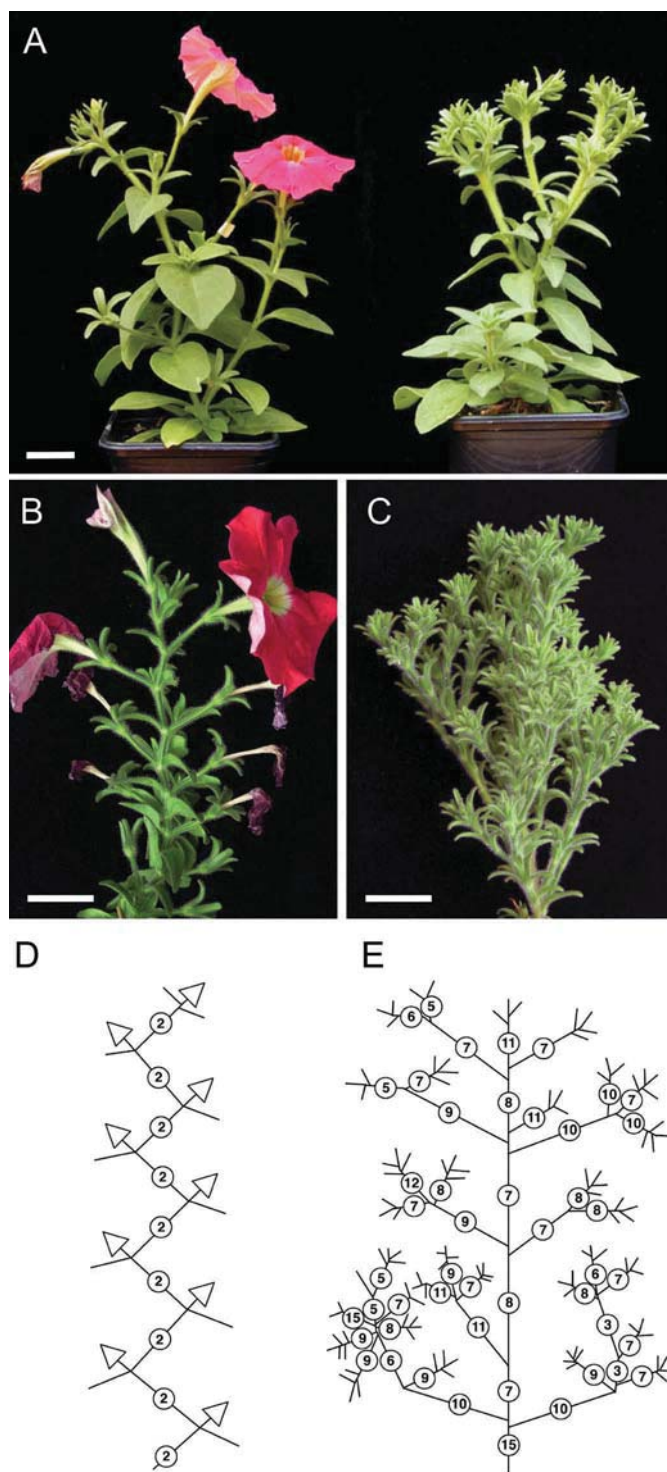
Figure 1. Mutant phenotype of *bns*. (A) Flowering wildtype W138 plant (left), and *bns* mutant (right) at the same age. (B) An advanced wildtype inflorescence with the characteristic zigzag inflorescence pattern. (C) An advanced *bns* inflorescence with the characteristic reiterative branching pattern and with abundant bract formation. (D) Schematic representation of a wildtype petunia inflorescence as in (B). (E) Schematic representation of a representative *bns* inflorescence. Numbers in (D,E) indicate the numbers of bracts between nodes. Size bars: 2 cm.

whereas the production of flowers is blocked in the mutants. In this sense, *bns* mutants resemble the phenotype of the *aberrant leaf and flower* (*alf*) mutant in petunia,[13] as well as the *leafy* mutant in *Arabidopsis thaliana*[15] and the *floricaula*
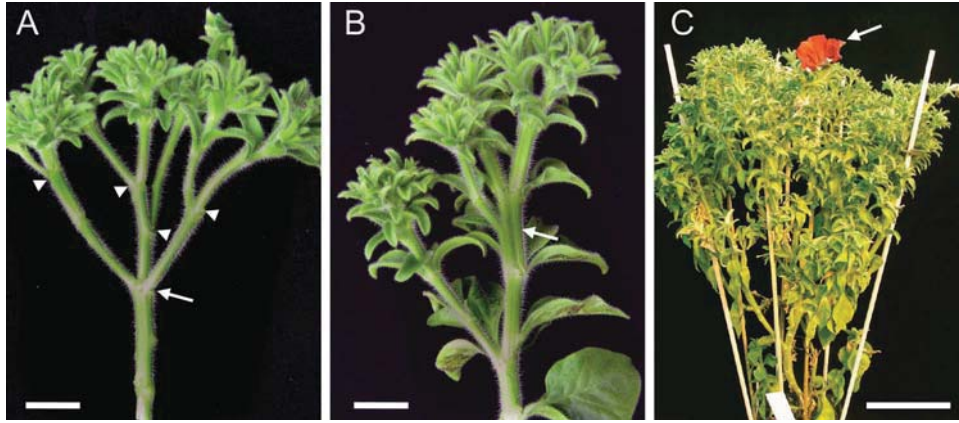
Figure 2. Branching pattern and reversibility of the *bns* phenotype. (A) After removal of the bracts, the branching pattern is revealed with repetitive lateral branching (arrowheads), and the formation of pseudo-whorls (arrow). (B) Formation of fasciated shoots in a *bns* inflorescence (arrow). (C) Rare event of flower formation in an old *bns* inflorescence (arrow). Size bars: 1 cm in (A), (B), 5 cm in (C).

mutant in *Antirrhinum majus*.[16] The *bns* mutants segregated 3:1 (wildtype:mutant) in a segregating population, and in the progeny of heterozygous mutants, indicating that the *bns* phenotype represents a monogenic recessive trait.

Shoot structure and phenotypic reversion in bns mutants

Closer inspection of shoot structure revealed several abnormalities in the mutants. In particular, *bns* plants produced pseudo-whorls (Figure 2A) and fasciated shoots (Figure 2B), indicating that the rate or organogenesis, and meristem size could be affected in *bns* mutants. After extended periods of growth, rare flowers were formed on *bns* mutants (Figure 2C), suggesting that the *bns* mutation is unstable and may be caused by a transposable element.

Revertant flowers were consistently overly large with increased numbers of floral organs (Figure 3). Instead of 5 sepals, 5 petals, 5 stamens and 2 carpels, the revertant flowers exhibited in the range of 8–12 sepals, petals and stamens (Figure 3A,C, compare with Figure 3B, D), and the number of carpels was often increased as well (Figure 3E). Many revertant flowers remained single, indicating that the revertant sector was entirely incorporated in the flower, and did not extend into the adjacent IM. However, in some cases, revertant flowers were accompanied by entire revertant inflorescence branches. On such branches, the first two flowers were abnormal, but the third flower was indistinguishable from the wildtype (Figure 3F). Taken together, these results strongly suggest that the *bns* mutation is caused by a transposon insertion.

### Development of wildtype inflorescence apices

The extreme fasciation of revertant flowers (Figure 3) suggests that meristem size may be increased in *bns* mutants. Before assessing meristem anatomy in *bns*, we first analyzed the reiterative sympodial branching pattern of the parental wild type line W138 (Figure 4). Petunia inflorescences undergo repetitive termination of the apical meristem in a flower and re-initiation of a new IM at its flank.[2,4] The new IMs undergo a stereotyped developmental program before they terminate in FMs themselves. First, the IM forms two bracts (Figure 4A). Then, a new IM is initiated in the axil of the second bract (Figure 4B), while the original IM is gradually transformed into an FM (Figure 4C), which starts to generate sepals in a spiral order (Figure 4D). Soon after this stage, the new IM will initiate two new bracts on its own and complete the next sympodial cycle by terminating in a flower, and by initiating a new lateral IM.

Bns meristems are enlarged and lack features of floral meristems

Bns mutant apices formed only leafy bracts in a spiral pattern (Figure 5A). New lateral shoots were not initiated in the axils of the youngest bracts as in the wildtype (see Figure 4), but in the axils of older bracts (Figure 5B) as in the case of the lateral shoots of vegetative apices. The axillary meristems acquired the same leafy identity as the main axis (Figure 5C), resulting in the highly branched leafy shoots shown in Figure 1C. Based on the fasciated stems and the highly fasciated revertant flowers, we tested whether *bns* mutants had enlarged meristems. Indeed, the main meristems were significantly larger than any wildtype meristems (Figure 5D). The lateral *bns* apices had the size of wt floral meristems, but were larger than wildtype IMs (Figure 5D). Comparing the lateral meristems of the two genotypes, we estimated that the volume of *bns* meristems corresponds to approximately 2.5-fold the volume of wild type inflorescence meristems. These results indicate that the indeterminate IM of *bns* mutants accumulate excess meristematic cells due to the lack of meristem splitting. It is conceivable that petunia has evolved a relaxed control over IM size, compared to monopodial plants, since wildtype IMs only have a very short developmental fate in the course of a sympodial cycle (Figure 4), thereby precluding the accumulation of excess meristematic cells. Interestingly, flower formation in revertant branches gradually reverted from fasciated flowers to normal flowers (Figure 3F), indicating that sympodial branching helps to regulate meristem size.
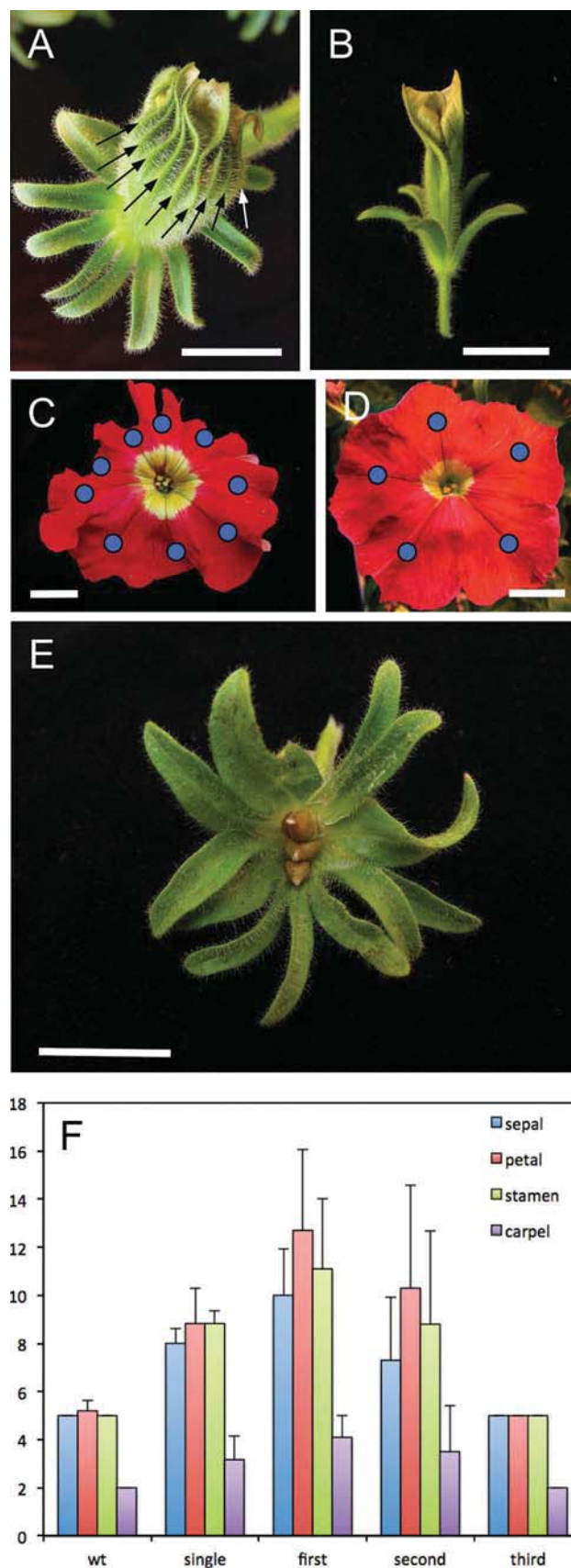
Figure 3. Phenotype of *bns* revertant flowers. (A) A *bns* revertant flower with increased numbers of sepals (10 visible), and a large corolla with many fused petals (arrows; 9 visible). (B) Wildtype flower at the same developmental stage as in (A). (C) A fully expanded *bns* revertant flower with 9 petals (marked by blue dots). (D) A representative wildtype flower at the same stage as in (C). (E) *Bns* mutant flower with 12 sepals and three separate fruit capsules (each consisting of two carpels). (F) Quantification of *bns* revertant flowers in comparison to wild type controls. *Bns* revertant flowers either appeared singly (single), or on revertant branches that carried several flowers (first, second, third). Size bars: 1 cm.
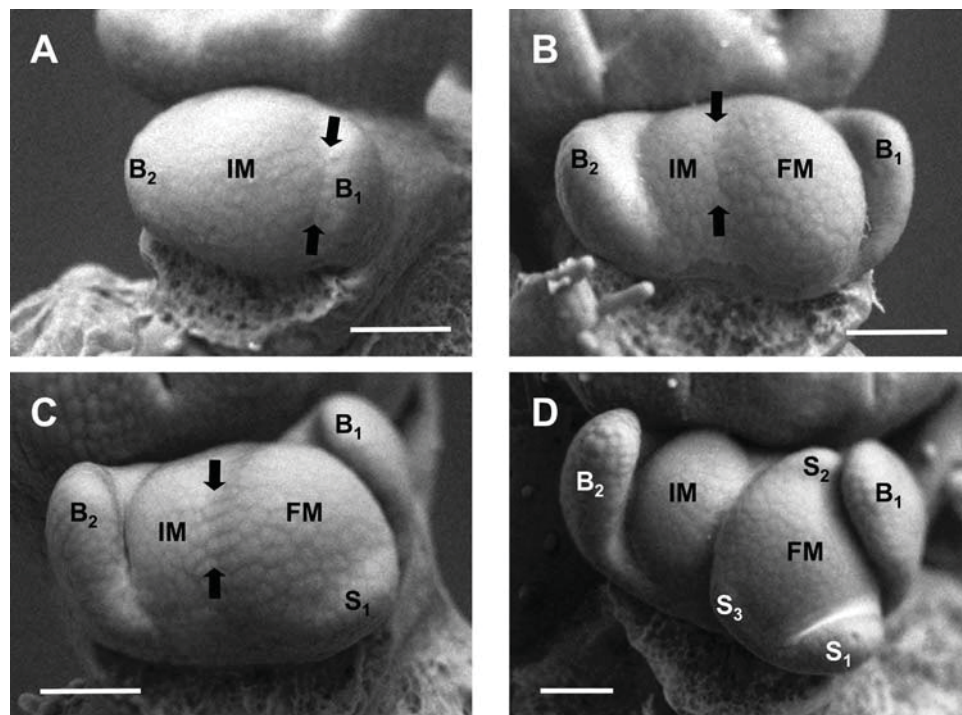
Figure 4. Development of wildtype sympodial inflorescence meristems. (A) Inflorescence meristem (IM) just after initiation of the two bracts (B1 and B2). B1 is already separated from the IM by a trough (arrows), showing that it is more advanced than B2. (B) Advanced sympodial unit that has started to initiate a new IM in the axil of B2, while the remainder of the original IM differentiates into a floral meristem (FM). The two meristems are already visibly separated by a through (arrows). (C) Sympodial unit with two bracts (B1 and B2), and a clearly separated new IM. The FM has already initiated the first sepal (S1). (D) Inflorescence apex as in (C) at an advanced stage. The FM has initiated a total of three sepals (S1-S3). Size bars: 50 μm.
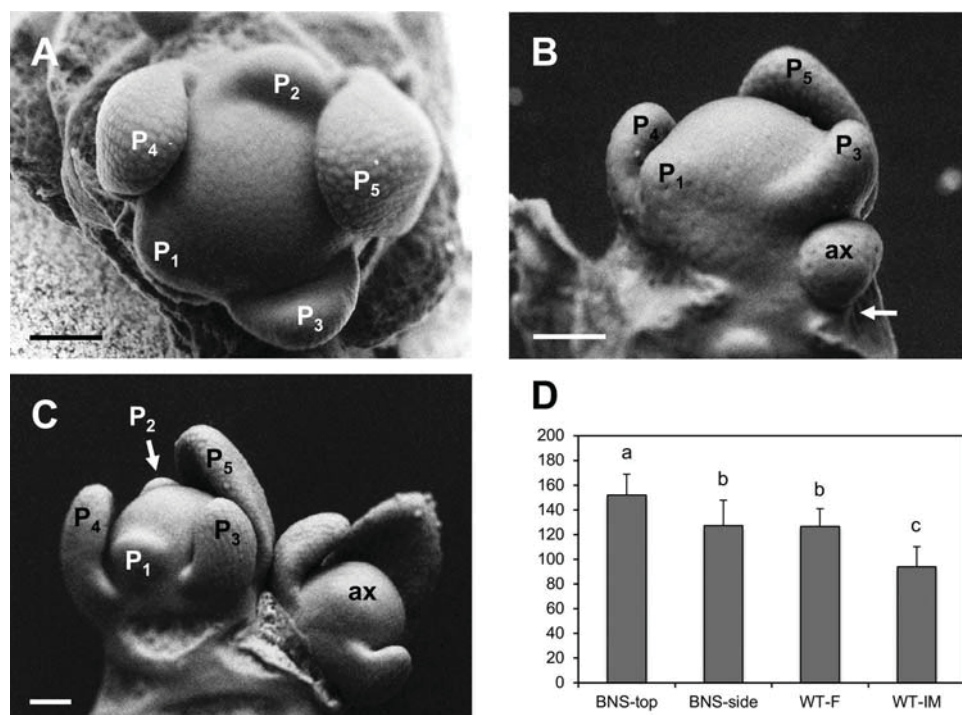
Figure 5. Development of the shoot apex in *bns* mutants. (A) The shoot apical meristem in *bns* mutants carries several leaf primordia in spiral succession (P_5-P_1). (B) Apex as in (A) from the side. Note the formation of an axillary bud (ax) from a subtending leaf axil (arrow). (C) Main shoot apex and subtending axillary bud at a further step of development. The axillary bud (ax) recapitulates the vegetative fate of the main shoot apical meristem. (D) Quantification of meristem diameter in *bns* apical meristems (*bns*-top), axillary meristems of *bns* mutants (*bns*-side), or floral meristems (WT-FM) and inflorescence meristem (WT-IM) of wildtype plants. Columns represent the average ± s.d. (n = 7). Values with different letters are significantly different (p < 0.05; Student's t-test). Size bars: 50 μm.

Root development in bns mutants

Since the shoot meristems were strongly affected by the *bns* mutation, it seemed appropriate to test whether root development was affected as well. First, the growth rate of the primary root was assessed for wild type and *bns* mutants in vertical plates with MS medium. In general, growth of *bns* mutants appeared to be slightly slower than in the wildtype, however, this difference was not significant (**Fig. S1**). After 11 days of growth, the vertical plates were rotated by 90° in order to assess the gravitropic response of *bns* and wildtype seedlings. After 1 day, wildtype plants had reoriented the root tip by 55.6° ± 13.1°, whereas *bns* mutant roots had been reoriented by 52.6° ± 11.6°, thus, no difference in the root gravitropic response was observed. Taken together, these results indicate that *BNS* has no function in the development of the root system.

Bns mutants have a dtph1 insertion in the EVERGREEN gene

The genetic basis of shoot development has been extensively studied in *P. hybrida*,[2] and some mutants, in particular *aberrant leaf and flower* (*alf*), *double top* (*dot*), and *evergreen* (*evg*) exhibit phenotypic similarities to the *bns* mutant.[13,17,18] Hence, genomic DNA from *bns* mutants was tested by PCR for insertions in these genes, and indeed, an insertion of a *dTPh1* transposable element was identified in the *EVERGREEN* (*EVG*) gene after nucleotide 121 downstream of the ATG start codon (**Fig. S2**). *EVG* encodes a WUSCHEL-LIKE HOMEOBOX (WOX) transcription factor of the WOX9 subfamily.[10,17] The transposon insertion in *bns* truncates the EVG protein upstream of the homeodomain (**Fig. S3a**), conceivably causing it to be a null allele. By comparison, the original *evg* allele has a *dTPh1* insertion downstream of the homeodomain (**Fig. S3a**).[17] In order to confirm the conclusion that the *bns* mutant phenotype is due to the *dTPh1* insertion in the *EVG* gene, we isolated and sequenced the *evg* locus of two independent *bns* revertant branches that gave rise to fertile flowers, indicating that they harbored a stable gene reversion. Indeed, in both cases, the transposon had excised and left a footprint of 6 bp, which restored the reading frame and resulted in the insertion of two additional amino acids (**Fig. S3b**).

EVG homologues have duplicated independently in diverse angiosperms

EVG has a close homologue in petunia, *SISTER OF EVG* (*SOE*).[17] Expression of *SOE* is highest during embryogenesis, in vegetative meristems, and in ovaries,[17] an expression pattern that resembles more the expression of its closest *Arabidopsis* homologue *STIMPY* (*STIP*), also known as *WOX9*[19] than the expression pattern of *EVG*.[17] *STIP* has no role in flower development, but regulates cell proliferation during embryogenesis and in vegetative meristems.[19] To explore the phylogenetic relationships between *EVG, STIP*, and their *WOX9*-like homologues in other angiosperms, and to see whether the duplication of *EVG* in petunia is a common feature in angiosperms, we retrieved the closest *EVG* homologues in various plants and compared their predicted amino acid sequences.

Besides petunia, we explored the genomes of the Solanaceous species tomato (*Solanum lycopersicum*) and potato (*Solanum tuberosum*), the legume model species *Medicago truncatula* and *Phaseolus vulgaris*, as well as grapevine (*Vitis vinifera*), poplar (*Populus trichocarpa*), and oilseed rape (*Brassica napus*). For comparison, we also included the monocot crops rice (*Oryza sativa*), and maize (*Zea mays*), and as outgroups, the closest homologues from the moss *Physcomitrella patens* and from the liverwort *Marchantia polymorpha*. We then identified in all species the *EVG* homologue(s) that were at least as closely related to *EVG* as the *Arabidopsis* gene *STIP-LIKE* (*STPL*) (also known as *WOX8*). For phylogenetic analysis, we also included AtWOX11 and AtWOX12,[20] which served to highlight the neighboring WOX subfamilies.

Based on these criteria, several of the species had two or even three EVG homologues (**Fig. S4**, colored dots), whereas several others had only one homologue (*Arabidopsis*, oilseed rape, grapevine, tomato, and potato). Since these are all well-characterized and complete genomes, we exclude the possibility to have missed or overlooked gene duplications in all these species. The duplications did not reveal a phylogenetic pattern that would indicate a common ancient gene duplication event in the ancestor of the evaluated species. Taken together, these results suggest that the *WOX9* homologues duplicated several times independently in a fraction of the analyzed plant species.

Deregulated gene expression patterns in bns mutants

Homeodomain transcription factors often act as master regulators that trigger developmental programs by transcriptional activation of regulatory cascades.[21] In order to assess the consequences of the mutation in the *EVG* gene on global transcriptional control, we performed microarray analysis using a custom-made microarray representing 24′816 unique petunia sequences.[22] Gene expression was compared between *bns* mutant apices and wildtype inflorescence apices, both normalized to young vegetative wild type apices.

Wild type inflorescence apices (including the smallest flower primordia) exhibited induction of 53 genes by more than 5-fold, of which 27 were induced more than 10-fold, relative to the vegetative apices (**Table S1**, Table 1). The 30 genes with the highest induction ratios encompassed 12 MADS-box genes that are known for their role in flower development[23,] (Table 1). In addition, the petunia *WUSCHEL/TERMINATOR* (*WUS/TER*) gene, and the floral regulator *DOUBLETOP* (*DOT*) were strongly induced in wild type inflorescence apices. In *bns* mutants, most of the flower-related MADS-box genes were not induced or even repressed relative to the vegetative control (Table 1). However, some genes that encode housekeeping functions of meristems such as a cyclin-dependent kinase, an RNA polymerase II-associated protein, and an ADP-ribose diphosphatase were induced both in wildtype inflorescences as in *bns* apices (Table 1). These genes are involved in the cell cycle and in cell growth, functions that are associated with active meristems, irrespective of their identity.

In order to reveal genes that may contribute to the *bns* phenotype, in particular to increased meristem size and lack of flowering, we determined genes that are induced in *bns* apices relative to the vegetative controls. Surprisingly, a total

6

of 548 genes were induced at least 5-fold, of which 199 were induced more than 10-fold relative to the vegetative wild type seedlings (**Table S2**). Strikingly, only 11 genes among the 548 *bns*-induced genes were also induced in the floral wild type apices indicating that the two meristem types have very different identities. Among the seven genes that were induced > 100-fold in *bns*, the highest one was the MADS-box gene *FBP13* (Table 2). This gene is expressed exclusively in vegetative organs,[24] and can therefore be regarded as a marker of vegetative tissues, although its function is elusive, since it has not been explored by mutant analysis. Taken together, these results show that *bns* apices are characterized by a general deregulation of gene expression and a vegetative identity.

Discussion

Monopodial and sympodial inflorescence development

Sympodial branching systems are characteristic for the inflorescence architecture of the Solanaceae, where they occur in a wide diversity.[2–4] In contrast to monopodial inflorescences, which are produced as continuous structures by a single indeterminate apical IM, sympodial inflorescences are composed of multiple metameric units, each consisting of a defined number of leafy structures that are produced by an inflorescence meristem before it terminates in a flower. These metamers are referred to as sympodial units. What characterizes the global appearance of sympodial inflorescences is the number and composition of individual sympodial units. In petunia, a sympodial unit consists of two bracts and a flower (Figure 4), and the number of sympodial units in an inflorescence is virtually unlimited (Figure 1B,D).[2,11] Hence, sympodial development is characterized by precisely regulated transitions between IM and FM identity, repeated initiation of new IMs, and fine-tuned control of meristem determinacy.

Role of EVERGREEN in acquisition of floral identity, meristem determinacy, and meristem size

Bns mutants have three major defects: a block in the establishment of floral identity, a defect in sympodial branching, and an accumulation of excess meristematic cells. These three phenomena are likely to be causally linked since acquisition of floral identity is connected with the loss of IM determinacy in sympodial plants. The lack of floral induction, thus, inevitably results in IM indeterminacy and defective sympodial branching. Hence, we propose that the failure to establish floral identity is the primary cause of the *bns* phenotype, and the other pleiotropic aspects of the phenotype are its consequences. Increased meristem size and fasciation may result as well from the defect in flowering. Since IMs are very short-lived in sympodial plants, and therefore are unlikely to overgrow under natural conditions, they may have a more relaxed size control mechanism than monopodial plants such as *Arabidopsis*.

Transcript profiling showed that MADS-box genes associated with flowering failed to become induced in *bns* mutant apices (Table 1). Whether these genes are direct targets of EVG, or whether they failed to become induced as a secondary consequence of the lack of floral transition in *bns* apices is unknown. On the other hand, the fact that hundreds of genes became ectopically induced in *bns* meristems (**Table S2**) indicates that one function of EVG could be to repress, directly or indirectly, genes that could potentially interfere with flower formation.

Evolution of inflorescence branching systems in the angiosperms

Based on the prevalence of monopodial branching systems among the angiosperms, it appears that sympodial branching may represent a derived condition that has evolved from monopodial systems. A conceptual scenario to explain the evolutionary transition from monopodial to sympodial systems is a progressive loss of indeterminacy in the apical IM, and the concomitant gain of indeterminacy in the lateral meristems (which in monopodial systems directly acquire floral identity). Support for a common evolutionary origin of monopodial and sympodial branching systems comes from the fact that most genes that have been identified as regulators of flowering in the monopodial model species *Arabidopsis thaliana* and *Antirrhinum maius* (snapdragon) have close homologues in sympodial model species such as petunia (*P. hybrida*), tomato (*S. lycopersicum*), and pepper (*C. annuum*), or in pea (*Pisum sativum*) that forms multiple inflorescences as lateral branches of a monopodial shoot.[25] In order to assess the degree of functional conservation among the conserved flower-related genes from monopodial and sympodial species, we identified the closest homologues of *EVG, LFY, UFO, STM, WUS, FT, AP1, SVP*, and *TFL1* from petunia, tomato, pea, snapdragon, and *Arabidopsis*, and we compared their function based on their mutant phenotypes described in the literature (**Table S3**).

Functional conservation and diversification of genes involved in flowering

The cross-species comparison revealed that several regulators of FM identity are functionally conserved among mono- and sympodial plants. For example, the floral switch *ALF* has a similar role in petunia as its orthologues in tomato (*FALSIFLORA; FA*), *Arabidopsis* (*LEAFY; LFY*), and *Antirrhinum* (*FLORICAULA; FLO*), since they all trigger the acquisition of FM identity in these divergent angiosperm species[26] (**Table S3**). Similarly, the function of the orthologous group represented by the petunia *DOUBLE TOP* (*DOT*),[18] the tomato *ANANTHA* (*AN*),[27] the *Antirrhinum FIMBRIATA* (*FIM*),[28] and the *Arabidopsis UNUSAL FLORAL ORGANS* (*UFO*) genes[29,30] is conserved since they all promote FM identity, although their mutant phenotypes are weaker in *Arabidopsis* and *Antirrhinum*[28–30] than in the other species (**Table S3**). Furthermore, the three orthologous groups containing the *Arabidopsis* genes *SHOOT MERISTEMLESS, WUSCHEL*, and *FLOWERING LOCUS T*, play functionally well conserved regulatory roles in meristem identity and activity (**Table S3**).

In contrast, the function of *EVG* and its closest homologues in other species (further collectively referred to as *WOX9* group) is highly divergent among the five angiosperm species compared here (**Table S3**). In *Arabidopsis*, the closest homologue (*STIMPY; STIP*) regulates cell proliferation in the embryo and

Table 1. Genes induced in wild type floral apices relative to vegetative apices (wt/veg), and their respective expression in *bns* mutant apices (bns/veg).

| Array sequence ID	P. axillaris gene ID	Function	functional class	Ratio wt/veg	Ratio bns/veg	Gene names
cn80	Peaxi162Scf00922g00026.1	MADS-box transcription factor	VIII. Gene expression and RNA metabolism	59.81	0.36	MADS (PhFBP1)
cn1378	Peaxi162Scf00175g00528.1		XIII. No homology	47.15	1.04	
GO_dr004P0022M20	nd	Anthranilate N-benzoyltransferase	VIa. Secondary metabolism	33.39	1.08	
GO_dr001P0017G22	Peaxi162Scf00247g00049.1	cyclin dependent kinase	XI. Cell cycle	32.35	23.72	
cn2931	Peaxi162Scf00020g02338.1	MADS-box transcription factor	VIII. Gene expression and RNA metabolism	25.89	0.31	MADS (PhMADS12)
GO_dr004P0001M11	Peaxi162Scf00271g00054.1	anthranilate N-hydroxycinnamoyl/benzoyltransferase	VIa. Secondary metabolism	25.68	0.75	
GO_drs12P0025F04	nd		XIII. No homology	23.29	21.71	
cn748	Peaxi162Scf00017g03246.1	MADS-box transcription factor	VIII. Gene expression and RNA metabolism	21.59	0.26	MADS (PhFBP23)
cn990	Peaxi162Scf00026g00144.1	transcription factor	VIII. Gene expression and RNA metabolism	21.57	0.44	PhCRABS CLAW
cn435	Peaxi162Scf00591g00074.1	Floral homeotic protein PMADS	VIII. Gene expression and RNA metabolism	21.31	0.12	PhFBP3
EB174737_1	Peaxi162Scf01241g00012.1		XIII. No homology	18.79	0.36	
GO_dr001P0009D10	nd	14-3-3 protein	X. Signalling	17.35	1.12	
cn1613	nd		XIII. No homology	16.04	1.07	
cn3359	Peaxi162Scf00021g00015.1	MADS-box transcription factor	VIII. Gene expression and RNA metabolism	14.65	0.46	MADS (PhMADS4)
cn716	Peaxi162Scf00128g01417.1	MADS-box transcription factor	VIII. Gene expression and RNA metabolism	13.80	0.08	MADS (PhFBP2)
cn1066	Peaxi162Scf00481g00721.1	MADS-box transcription factor	VIII. Gene expression and RNA metabolism	13.74	0.09	MADS (PhFBP5)
cn747	Peaxi162Scf00365g00212.1	MADS-box transcription factor	VIII. Gene expression and RNA metabolism	13.53	0.33	MADS (PhFBP9)
cn4960	Peaxi162Scf00516g00125.1	nodulin MtN3 family protein	XIIa. Biotic stimuli	13.26	1.15	
GO_dr001P0020C09	Peaxi162Scf00362g00356.1	RNA polymerase II-associated protein	VIII. Gene expression and RNA metabolism	12.71	14.70	
cn704	Peaxi162Scf01084g00119.1	MADS-box transcription factor	VIII. Gene expression and RNA metabolism	12.69	0.08	MADS (Green petals)
cn2934	Peaxi162Scf00154g00516.1	MADS-box transcription factor	VIII. Gene expression and RNA metabolism	12.58	0.35	MADS (PhFBP6)
GO_dr001P0001C02	nd		XIII. No homology	12.24	1.59	
cn79	nd		XIII. No homology	12.23	0.36	
GO_dr004P0001K16	Peaxi162Scf00300g10017.1		XIII. No homology	11.48	0.72	
IP_PHBS005O01u	Peaxi162Scf00802g00122.1	ADP-ribose diphosphatase/ NAD binding / hydrolase	Va. Primary metabolism	10.98	13.34	
cn300	Peaxi162Scf00022g00098.1	MADS-box transcription factor	VIII. Gene expression and RNA metabolism	10.41	0.21	MADS (PhMADS3)
GO_dr004P0017J19	nd	predicted protein	XIId. Unknown	10.23	7.48	
GI_NP1239971	Peaxi162Scf00083g00516.1	WUSCHEL; transcription factor	VIII. Gene expression and RNA metabolism	9.95	1.82	WUS
GI_NP1240120	Peaxi162Scf00688g00335.1	MADS-box transcription factor	VIII. Gene expression and RNA metabolism	9.16	0.95	MADS (PhFBP11)
cn933	Peaxi162Scf00099g01816.1		XIII. No homology	8.10	8.14	
GO_drpoolB-CL6341Contig1	Peaxi162Scf01284g00017.1		XIII. No homology	7.58	12.59	
GO_dr004P0010F08	Peaxi162Scf00241g00053.1	invertase/pectin methylesterase inhibitor family protein	Ia. Cell wall	7.26	3.27	
cn10000	Peaxi162Scf00048g00175.1	ubiquitin-protein ligase DOT	IX. Protein synthesis, processing and degradation	7.04	0.14	DOT
cn4557	nd	lipid transfer protein	XII. Miscellaneous	6.51	4.10	
cn9095	nd	double-stranded RNA binding protein	XII. Miscellaneous	6.38	4.79	
cn1805	nd	S-adenosyl-L-methionine synthase	Va. Primary metabolism	5.93	4.94	
EB174854_1	nd		XIII. No homology	5.72	5.22	
cn2222	Peaxi162Scf00297g00816.1	gamma-thionin	XIIa. Biotic stimuli	5.71	3.06	
cn2225	nd	gamma-thionin	XIIa. Biotic stimuli	5.58	1.00	
GO_dr004P0029J18	Peaxi162Scf00270g00108.1	PYRIDOXINE BIOSYNTHESIS 2; glutaminase/ glutaminyl-tRNA synthase	Va. Primary metabolism	5.44	1.36	
GO_dr004P0013G04	Peaxi162Scf00420g00252.1	predicted protein	XIId. Unknown	5.42	0.95	
cn5911	Peaxi162Scf00347g00822.1	protein transport protein sec22	IVb. Vesicular trafficking secretion and protein sorting	5.41	6.60	
DC240060_1	nd		XIII. No homology	5.35	1.00	
GO_dr004P0009C08	Peaxi162Scf00064g00912.1	UDP-glucosyltransferase	VIa. Secondary metabolism	5.30	27.54	
cn8613	nd	bZIP family transcription factor	VIII. Gene expression and RNA metabolism	5.25	1.89	
cn1107	nd	Photosystem I subunit	Va. Primary metabolism	5.24	5.90	
EB174538_1	Peaxi162Scf00535g00016.1	eukaryotic transcription factor	VIII. Gene expression and RNA metabolism	5.21	1.67	
GI_TC1170	Peaxi162Scf00083g01812.1	MADS-box transcription factor	VIII. Gene expression and RNA metabolism	5.19	1.11	MADS
GO_dr004P0012K11	Peaxi162Scf00253g00619.1	phosphatidylethanolamine binding	IVa. Membrane constituents (phospholipids, sterols etc.)	5.14	1.41	
cn4534	Peaxi162Scf00129g00133.1		XIII. No homology	5.08	3.23	
cn3083	Peaxi162Scf00007g02519.1	predicted protein	XIId. Unknown	5.05	1.86	

in the vegetative shoot meristems.[19] In *Antirrhinum* the corresponding orthologue has not been described to date, perhaps because its mutation does not cause a strong phenotype. Most strikingly, in the Solanaceous species tomato, the *WOX9* orthologue *COMPOUND INFLORESCENCE* (*S*) has no role in the acquisition of FM identity, but instead controls branching in the inflorescence.[27] In contrast, mutations in the *S* homologue of pepper (*Capsicum annuum S, CaS*) resemble more the *bns* phenotype than the defects in the tomato *s* mutant.[31] As in the case of the *WOX9* orthologues, the role of the petunia *EXP* gene and its closest homologues in the other model species are considerably different, ranging from regulation of IM indeterminacy (petunia) to timing of floral transition (*Arabidopsis*), fruit abscission (tomato) (**Table S3**), and to repression of vegetative fate (pepper).[32]

A model for the regulation of flowering in angiosperms

Based on our results and the analysis of Rebocho *et al.* (2008), and in the light of the comparison of functionally conserved vs. diversified elements involved in flowering (**Table S3**), we propose a model for the role of *EVG* in the induction of flowering (Figure 6). The model involves a series of events that lead to the transition from IM identity to FM identity. To a large degree, these events are controlled by functionally conserved proteins,

that therefore represent evolutionary stable nodes in the regulatory network (e.g. *ALF, DOT,* and *FT*). In contrast, *EVG* and *EXP* represent regulatory elements that have diverged considerably among angiosperms, and even within the Solanaceae, indicative of rapid evolution. The unexpected finding that the defect of *evg* in FM formation is restored by mutations in *HERMIT* (*HER*), or *EXTRAPETALS* (*EXP*)[17] can be explained by the operation of two mutually inhibitory pathways. The EVG pathway promotes floral identity, whereas the EXP/HER pathway ensures the maintenance of IM identity to avoid complete meristem termination (Figure 6). Since the expression of *DOT* in a *evg* mutant background is sufficient to restore FM identity,[17] *EVG* appears to act mainly through *DOT* to induce FM identity (in combination with its interactor ALF). The competitive interaction between the activity of *EVG* and the activity of *HER* and *EXP* can potentially result in the complete loss of FM identity (as in the *evg* mutant), or in complete acquisition of FM identity resulting in solitary flowers (in *her* and *exp* mutants). Thus, *EVG, HER* and *EXP* may represent central elements in the mechanism that balances meristem identity, both ontogenetically as well as evolutionarily.

According to the model, sympodial branching requires dynamic fine-tuning of the competing pathways represented by *EVG, HER* and *EXP* (Figure 6C). In the case of restored flower formation in *evg/exp* double mutants,[17] residual activity
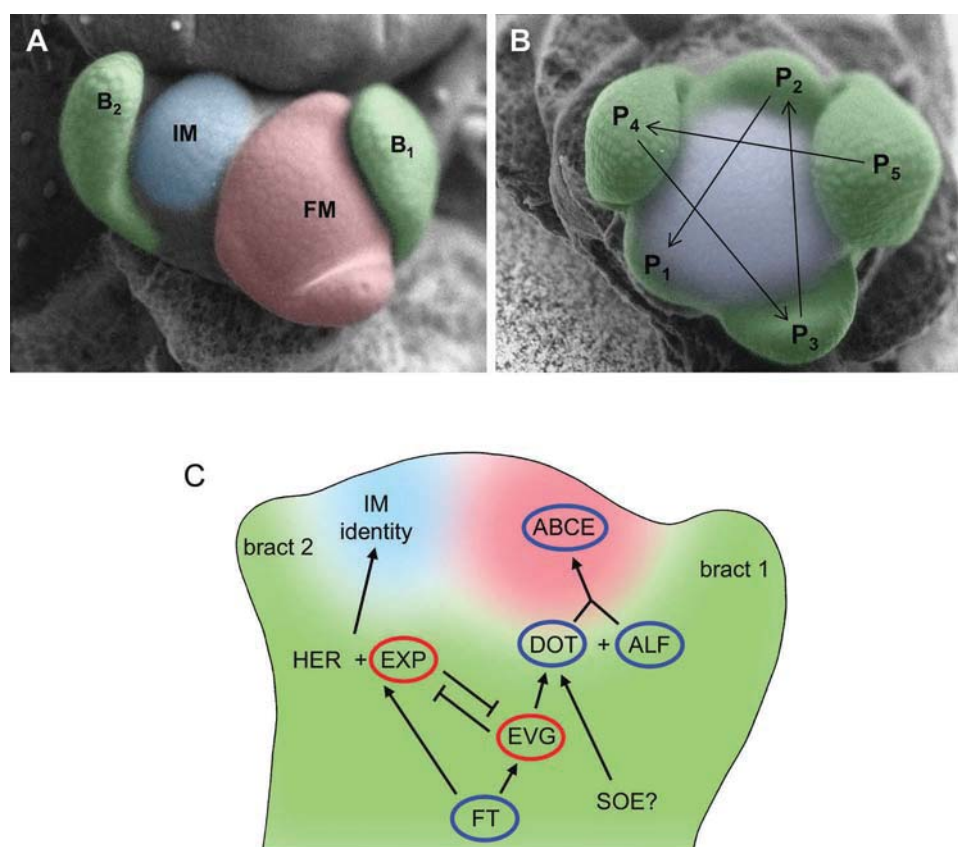
Figure 6. A model for the regulation of floral identity at the shoot apex. (A) Wildtype apex with 2 bracts (green), the flower meristem (red), and the inflorescence meristem (blue). (B) *Bns* apical meristem in top view with the youngest primordia in spiral succession, and the enlarged IM in the center (blue). Spiral phyllotaxis is indicated with arrows. (C) A model for the genetic regulation of flowering in petunia. At the onset of flowering, a floral signal (FT) initiates two competing pathways, the core floral pathway involving EVG and its downstream target DOT, and the constitutively expressed ALF. In parallel, an inhibitory pathway, involving EXP and HER is triggered which inhibits floral fate locally, and thereby promotes IM identity. Functionally conserved elements are highlighted with blue circles, the less conserved elements (EVG and EXP) are highlighted in red (compare with Table S3). Note that arrows do not necessarily reflect direct regulation.

of *SOE* or another redundant gene may allow solitary flower formation. How sensitive this regulatory node is towards disturbance is illustrated by the surprising fact that crossing the *evg* allele from W138 into the *P. hybrida* genetic background W115 resulted in a wide phenotypic diversity in the F2. Homozygous *evg* mutants showed either the original *evg* phenotype (lack of flowers), or the opposite with solitary flowers (as in *her* or *exp* mutants), and a range of intermediate phenotypes.[17] This unexpected result shows that the regulatory node involving *EVG, HER,* and *EXP* represents an exceptionally sensitive regulatory node.

Conclusion

We confirm earlier reports that have assigned a central role for the petunia *WOX9* homologue *EVG* in the acquisition of floral identity in petunia (Figures 1 and 5),[17] and we show that mutation of EVG leads to a fundamental deregulation of gene expression in the shoot apex (Table 1; **Table S1**; Table 2; **Table S2**). While highly conserved regulatory components such as the floral inducer *FT* and the downstream regulators *DOT* and *ALF*, have similar roles in the angiosperm species compared here, *EVG* and other *WOX9* homologues play divergent roles in angiosperm flowering. Thus, *WOX9* homologues may represent sensitive regulatory nodes that could have been important drivers in the evolution of branching architecture by acting as a "meristem maturation clock".[33] Thus, *WOX9* gene duplications (such as *EVG* and *SOE*), alterations in the expression patterns of *WOX9* members, and functional diversification of the encoded proteins may have provided the substrate for "fine-tuning" of IM and FM fate during the evolution of the Solanaceae to give rise to the enormous diversity of the sympodial inflorescences in the Solanaceae.[3,4]

Materials and methods

Plant growth conditions and mutant screen

Plants (*Petunia hybrida* line W138) were grown as described.[34] Briefly, seeds were germinated on seedling substrate (Klasmann, http://www.klasmann-deilmann.com), and after four weeks, plantlets were transferred to pots (ca. 150 ml) with clay substrate (Klasmann, http://www.klasmann-deilmann.com). Mutants with defects in flower development were screened phenotypically in families of eight as described.[35] In case of interesting phenotypes, 40 additional plants were grown from the same family to establish segregation patterns.

Microscopy

Scanning electron microscopy was performed with an S-3500N variable pressure scanning electron microscope from Hitachi (Tokyo, Japan), equipped with a cool stage as described.[36,37]

Gene expression analysis

Gene expression analysis was performed by hybridisation of fluorescently labelled cDNA to custom-made petunia microarrays by Nimblegen as described.[22,34] Briefly, ca. 500 apices of wildtype inflorescences apices, *bns* mutant apices and vegetative wildtype apices were collected and stored in 70% ethanol (vol/ vol). Total root RNA was extracted with the hot phenol procedure,[38] and sent to Nimblegen on dry ice for microarray analysis. Array design of a four-plex microarray with 72′000 features was carried out using the Array-Scribe software from NimbleGen (http://www.nimblegen.com) to generate three optimized independent probes per gene, with an average length of 36 base pairs per probe. Array design, probe synthesis, synthesis of labeled cDNA, hybridization, and data acquisition was carried out by Nimblegen as described.[39] Average expression values and a coefficient of variation for the gene expression values were derived by across-array quantile normalization using the Robust Multichip Average (RMA) algorithm.[40] Comparative analysis of expression data sets was carried out with Fire2.2[41] according to the instructions from the authors.

Root growth assay

For root growth analysis, seedlings were grown on 1/2 strength MS medium without sugar on square vertical plates. The root tips were marked on the bottom of the plates at regular intervals (4d, 7d, 11d) after transfer to the medium. Gravitropic stimulation was performed by turning the plates by 90 degree, whereby the seedlings were oriented horizontally.

Measurements of meristem size

In order to measure the diameter of various meristems in petunia wildtype and *bns* mutants, apices were imaged by SEM (see above), and meristem size was measured from the pictures after calibration of the image size.

Isolation of the bns mutant allele

Mutant DNA from *bns* leaves, or from revertant branches, was amplified with forward primer EVG-F13 (ATGGCATCA TCAAATAGACATTGG), and with out7 (GGGCTCACC ACCCAGGATC). The resulting amplicon was cloned into pGEMT easy and sequenced, and revealed the site of *dTPh1* insertion after nucleotide 121 of the coding region.

Phylogenetic analysis

To retrieve the homologues of known flower-related genes, the predicted protein sequences of the petunia flower-related genes ALF, DOT, HER, WUS/TER, PehFT, EVG, and EXP were used for tblastn searches in NCBI (https://www.ncbi.nlm.nih.gov) and on SolGenomics (https://solgenomics.net). To confirm orthology, the corresponding searches were also performed with the closest homologues from *Arabidopsis thaliana* and *Antirrhinum majus*. In the case of *SELF PRUNING (SP), CENTRORADIALIS (CEN)*, and *TERMINAL FLOWER1 (TFL1)*, the tomato sequence was used instead of the petunia sequence.

For phylogenetic analysis of EVG with other WOX9-related genes, the EVG protein sequence was used to search the angiosperm database by blastp. The first few hits per species were used for initial phylogenetic analysis. In order to test for duplications of WOX9/EVG homologues, sequences that were at least as

Table 2. Genes induced in *bns* apices relative to vegetative apices (bns/veg), and their respective expression in wild type floral apices (wt/veg).

Array sequence ID	P. axillaris gene ID	Function	functional class	Ratio wt/veg	Ratio bns/veg	Gene names
cn80	Peaxi162Scf00922g00026.1	MADS-box transcription factor (FBP13)	VIII. Gene expression and RNA metabolism	1.90	291.80	FBP13
cn1378	Peaxi162Scf00175g00528.1		XIII. No homology	1.06	205.47	
GO_dr004P0022M20	nd	invertase inhibitor	Va. Primary metabolism	1.88	157.39	
GO_dr001P0017G22	Peaxi162Scf00247g00049.1	sulfate transporter	IIIb. Mineral nutrient responsive and aquisition	2.63	122.84	
cn2931	Peaxi162Scf00020g02338.1		XIII. No homology	1.02	120.65	
GO_dr004P0001M15	Peaxi162Scf00271g00054.1	metallothionein-like protein	XIIb. Abiotic stimuli	1.77	116.91	
GO_drs12P0025F04	nd	peroxidase	Vb. Antioxidative metabolism and Redox state	0.69	114.72	
cn748	Peaxi162Scf00017g03246.1	digalactosyldiacylglycerol synthase 2	Va. Primary metabolism	2.08	94.79	
cn990	Peaxi162Scf00026g00144.1		XIII. No homology	0.71	84.50	
cn435	Peaxi162Scf00591g00074.1	polygalacturonase	Ia. Cell wall	1.36	80.08	
EB174737_1	Peaxi162Scf01241g00012.1	Nicotianamine synthase	Va. Primary metabolism	2.57	76.23	
GO_dr001P0009D10	nd	Nicotianamine synthase	Va. Primary metabolism	1.78	73.23	
cn1613	nd	purine transmembrane transporter	IIIa. Membrane transport	2.37	72.91	
cn3359	Peaxi162Scf00021g00015.1	elicitor-inducible protein	XIIa. Biotic stimuli	0.55	71.66	
cn716	Peaxi162Scf00128g01417.1		XIII. No homology	1.32	68.95	
cn1066	Peaxi162Scf00481g00721.1		XIII. No homology	1.80	68.93	
cn747	Peaxi162Scf00365g00212.1		XIII. No homology	1.04	67.38	
cn4960	Peaxi162Scf00516g00125.1		XIII. No homology	1.08	66.34	
GO_dr001P0020C09	Peaxi162Scf00362g00356.1	gibberellin-induced protein	VIb4. Giberellin metabolism and perception	1.28	62.05	
cn704	Peaxi162Scf01084g00119.1	anionic peroxidase	Vb. Antioxidative metabolism and Redox state	1.01	59.64	
cn2934	Peaxi162Scf00154g00516.1	caspase	IX. Protein synthesis, processing and degradation	1.10	58.88	
GO_dr001P0001C02	nd		XIII. No homology	0.72	54.26	
cn79	nd	peroxidase	Vb. Antioxidative metabolism and Redox state	0.95	50.44	
GO_dr004P0001K16	Peaxi162Scf00300g10017.1	hyoscyamine 6 beta-hydroxylase	VIa. Secondary metabolism	2.84	48.97	
IP_PHBS005O01u	Peaxi162Scf00802g00122.1	sulfate transporter	IIIb. Mineral nutrient responsive and aquisition	1.56	48.43	
cn300	Peaxi162Scf00022g00098.1	5-methyltetrahydrofolate:homocysteine methyltransferase	Va. Primary metabolism	1.34	47.29	
GO_dr004P0017J19	nd		XIII. No homology	2.89	44.28	
GI_NP1239971	Peaxi162Scf00083g00516.1	nitrate transporter	IIIb. Mineral nutrient responsive and aquisition	1.02	43.90	
GI_NP1240120	Peaxi162Scf00688g00335.1		XIII. No homology	0.98	43.53	
cn933	Peaxi162Scf00099g01816.1		XIII. No homology	1.38	43.08	
GO_drpoolB-CL6341Contig1	Peaxi162Scf01284g00017.1	hemoglobin non-symbiotic	Vb. Antioxidative metabolism and Redox state	1.84	43.08	
GO_dr004P0010F08	Peaxi162Scf00241g00053.1	cell death associated protein	XIIc. Development and tissue specific	1.36	41.50	
cn10000	Peaxi162Scf00048g00175.1	peroxidase	Vb. Antioxidative metabolism and Redox state	0.87	41.41	
cn4557	nd		XIII. No homology	0.96	40.64	
cn9095	nd	metallothionein	XIIb. Abiotic stimuli	1.73	40.26	
cn1805	nd	HR7	IX. Protein synthesis, processing and degradation	0.97	40.22	
EB174854_1	nd	protease inhibitor/seed storage/lipid transfer protein family protein	XII. Miscellaneous	1.39	39.17	
cn2222	Peaxi162Scf00297g00816.1		XIII. No homology	1.49	38.95	
cn2225	nd	histone cluster 2	VII. Chromatin and DNA metabolism	1.60	38.07	
GO_dr004P0029J18	Peaxi162Scf00270g00108.1	ubiquitin conjugating enzyme	IX. Protein synthesis, processing and degradation	1.19	37.88	
GO_dr004P0013G04	Peaxi162Scf00420g00252.1	sulfate transporter	IIIb. Mineral nutrient responsive and aquisition	1.20	37.43	
cn5911	Peaxi162Scf00347g00822.1	transducin family protein / WD-40 repeat family protein	X. Signalling	0.83	36.41	
DC240060_1	nd	nodulin	XIIa. Biotic stimuli	0.92	36.19	
GO_dr004P0009C08	Peaxi162Scf00064g00912.1	hyoscyamine 6 beta-hydroxylase [Atropa baetica]	VIa. Secondary metabolism	1.79	35.93	
cn8613	nd	proline-rich protein	Ia. Cell wall	0.99	34.00	
cn1107	nd	PDR-type ABC transporter	IIIa. Membrane transport	1.89	32.82	
EB174538_1	Peaxi162Scf00535g00016.1	peroxidase	Vb. Antioxidative metabolism and Redox state	0.72	32.69	
GI_TC1170	Peaxi162Scf00083g01812.1	oxidoreductase	XII. Miscellaneous	1.24	32.58	
GO_dr004P0012K11	Peaxi162Scf00253g00619.1	caspase	IX. Protein synthesis, processing and degradation	0.96	32.40	
cn4534	Peaxi162Scf00129g00133.1	actin	II. Cytoskeleton	3.65	30.54	
cn3083	Peaxi162Scf00007g02519.1	tyrosine specific protein phosphatase	X. Signalling	1.68	29.68	

11

closely related to EVG as AtWOX8 were used for final phylogenetic analysis. AtWOX8, AtWOX11, and AtWOX12 were included to highlight the neighboring WOX subfamilies. Sequences used for tree construction (**Fig. S4**) are listed in **File S1**. Sequence comparison and generation of the phylogenetic tree with EVG homologues was carried out with the entire amino acid sequence using the "advanced" function of the software package at www.phylogeny.fr,[42] with 100 bootstrap replicates.

Abbreviations

FM   Floral meristem
IM   Inflorescence meristem
BNS   BONSAI
EVG   EVERGREEN
WUS   WUSCHEL
WOX   WUSCHEL-LIKE HOMEOBOX

Disclosure statement

No potential conflict of interest was reported by the authors.

Author contributions

M.S. and D.M.R.R. performed the experiments; D.R. conceived and supervised the project. A. F. performed bioinformatics analysis. All authors contributed to the interpretation of the results and the writing of the paper.

ORCID

R. R. Duvvuru Muni 🄳 http://orcid.org/0000-0001-6838-0482
A. Fiebig 🄳 http://orcid.org/0000-0003-3159-3593
Didier Reinhardt 🄳 http://orcid.org/0000-0003-3495-6783

References

1. Schmitz G, Theres K. Genetic control of branching in *Arabidopsis* and tomato. Curr Opin Plant Biol. 1999;2:51–55.
2. Castel R, Kusters E, Koes R. Inflorescence development in petunia: through the maze of botanical terminology. J Exp Bot. 2010;61:2235–2246. doi:10.1093/jxb/erq061.
3. Danert S. Die Verzweigung der Solanaceen im reproduktiven Bereich. Abh Deutsch Akad Wiss Berlin, Math-Naturwiss Kl 1957. 1958;6:1–184.
4. Reinhardt D, Kuhlemeier C. Plant architecture. EMBO Rep. 2002;3:846–851. doi:10.1093/embo-reports/kvf177.
5. Galli M, Gallavotti A. Expanding the reculatory network for meristem size in plants. Trends Genet. 2016;32:372–383.
6. Ha CM, Jun JH, Fletcher JC. Shoot apical meristem form and function. In: Timmermans MCP, ed. Plant development. 2010. San Diego (CA): Academic Press. p. 103–140.
7. Mayer KFX, Schoof H, Haecker A, Lenhard M, Jurgens G, Laux T. Role of *WUSCHEL* in regulating stem cell fate in the *Arabidopsis* shoot meristem. Cell. 1998;95:805–815.
8. Schoof H, Lenhard M, Haecker A, Mayer KFX, Jürgens G, Laux T. The stem cell population of *Arabidopsis* shoot meristems is maintained by a regulatory loop between the *CLAVATA* and *WUSCHEL* genes. Cell. 2000;100:635–644.
9. Somssich M, Je BI, Simon R, Jackson D. CLAVATA-WUSCHEL signaling in the shoot meristem. Development. 2016;143:3238–3248.
10. Costanzo E, Tréhin C, Vandenbussche M. The role of *WOX* genes in flower development. Ann Bot. 2014;114:1545–1553. doi:10.1093/aob/mcu123.
11. Rijpkema A, Gerats T, Vandenbussche M. Genetics of floral development in Petunia. Adv Bot Research: Inc Adv Plant Pathol. 2006;44:237–278.
12. Gerats T, Vandenbussche M. A model system for comparative research: petunia. Trends Plant Sci. 2005;10:251–256. doi:10.1016/j.tplants.2005.03.005.
13. Souer E, Van Der Krol A, Kloos D, Spelt C, Bliek M, Mol J, Koes R. Genetic control of branching pattern and floral identity during Petunia inflorescence development. Development. 1998;125:733–742.
14. Gerats AGM, Huits H, Vrijlandt E, Maraña C, Souer E, Beld M. Molecular characterization of a nonautonomous transposable element (dTph1) of petunia. Plant Cell. 1990;2:1121–1128.
15. Weigel D, Alvarez J, Smyth DR, Yanofsky MF, Meyerowitz EM. *LEAFY* controls floral meristem identity in *Arabidopsis*. Cell. 1992;69:843–859.
16. Coen ES, Romero JM, Doyle S, Elliott R, Murphy G, Carpenter R. *FLORICAULA* - a homeotic gene required for flower development in *Antirrhinum majus*. Cell. 1990;63:1311–1322.
17. Rebocho AB, Bliek M, Kusters E, Castel R, Procissi A, Roobeek I, Sour E, Koes R. Role of *EVERGREEN* in the development of the cymose petunia inflorescence. Dev Cell. 2008;15:437–447. doi:10.1016/j.devcel.2008.08.007.
18. Souer E, Rebocho AB, Bliek M, Kusters E, De Bruin RAM, Koes R. Patterning of inflorescences and flowers by the F-box protein DOUBLE TOP and the LEAFY homolog ABERRANT LEAF AND FLOWER of petunia. Plant Cell. 2008;20:2033–2048. doi:10.1105/tpc.108.060871.
19. Wu XL, Dabi T, Weigel D. Requirement of homeobox gene *STIMPY/WOX9* for *Arabidopsis* meristem growth and maintenance. Curr Biol. 2005;15:436–440. doi:10.1016/j.cub.2004.12.079.
20. Haecker A, Gross-Hardt R, Geiges B, Sarkar A, Breuninger H, Herrmann M, Laux T. Expression dynamics of *WOX* genes mark cell fate decisions during early embryonic patterning in *Arabidopsis thaliana*. Development. 2004;131:657–668. doi:10.1242/dev.00963.
21. Kaufmann K, Pajoro A, Angenent GC. Regulation of transcription in plants: mechanisms controlling developmental switches. Nat Rev Genet. 2010;11:830–842. doi:10.1038/nrg2885.
22. Breuillin F, Schramm J, Hajirezaei M, Ahkami A, Favre P, Druege U, Hause B, Bucher M, Kretzschmar T, Bossolini E, et al. Phosphate systemically inhibits development of arbuscular mycorrhiza in *Petunia hybrida* and represses genes involved in mycorrhizal functioning. Plant J. 2010;64:1002–1017. doi:10.1111/j.1365-313X.2010.04385.x.
23. Heijmans K, Morel P, Vandenbussche M. MADS-box genes and floral development: the dark side. J Exp Bot. 2012;63:5397–5404. doi:10.1093/jxb/ers233.

24. Immink RGH, Ferrario S, Busscher-Lange J, Kooiker M, Busscher M, Angenent GC. Analysis of the petunia MADS-box transcription factor family. Mol Genet Genomics. 2003;268:598–606. doi:10.1007/s00438-002-0781-3.

25. Berbel A, Ferrandiz C, Hecht V, Dalmais M, Lund OS, Sussmilch FC, Taylor SA, Bendahmane A, Ellis THN, Beltran JP, et al. VEGETATIVE1 is essential for development of the compound inflorescence in pea. Nat Commun. 2012;3. doi:10.1038/ncomms1801.

26. Benlloch R, Berbel A, Serrano-Mislata A, Madueno F. Floral initiation and inflorescence architecture: A comparative view. Ann Bot. 2007;100:659–676. doi:10.1093/aob/mcm146.

27. Lippman ZB, Cohen O, Alvarez JP, Abu-Abied M, Pekker I, Paran I, Eshed Y, Zamir D. The making of a compound inflorescence in tomato and related nightshades. PLoS Biol. 2008;6:2424–2435. doi:10.1371/journal.pbio.0060288.

28. Simon R, Carpenter R, Doyle S, Coen E. FIMBRIATA controls flower development by mediating between meristem and organ identity genes. Cell. 1994;78:99–107.

29. Ingram GC, Goodrich J, Wilkinson MD, Simon R, Haughn GW, Coen ES. Parallels between UNUSUAL FLORAL ORGANS and FIMBRIATA, genes controlling flower development in Arabidopsis and Antirrhinum. Plant Cell. 1995;7:1501–1510. doi:10.1105/tpc.7.9.1501.

30. Levin JZ, Meyerowitz EM. UFO - an Arabidopsis gene involved in both floral meristem and floral organ development. Plant Cell. 1995;7:529–548. doi:10.1105/tpc.7.5.529.

31. Cohen O, Borovsky Y, David-Schwartz R, Paran I. Capsicum annuum S (CaS) promotes reproductive transition and is required for flower formation in pepper (Capsicum annuum). New Phytol. 2014;202:1014–1023. doi:10.1111/nph.12711.

32. Cohen O, Borovsky Y, David-Schwartz R, Paran I. CaJOINTLESS is a MADS-box gene involved in suppression of vegetative growth in all shoot meristems in pepper. J Exp Bot. 2012;63:4947–4957. doi:10.1093/jxb/ers172.

33. Park SJ, Jiang K, Schatz MC, Lippman ZB. Rate of meristem maturation determines inflorescence architecture in tomato. Proc Natl Acad Sci U S A. 2012;109:639–644. doi:10.1073/pnas.1114963109.

34. Nouri E, Breuillin-Sessoms F, Feller U, Reinhardt D. Phosphorus and nitrogen regulate arbuscular mycorrhizal symbiosis in Petunia hybrida. PLoS ONE. 2014;9:e90841. doi:10.1371/journal.pone.0090841.

35. Sekhara Reddy DMR, Schorderet M, Feller U, Reinhardt D. A petunia mutant affected in intracellular accommodation and morphogenesis of arbuscular mycorrhizal fungi. Plant J. 2007;51:739–750. doi:10.1111/j.1365-313X.2007.03175.x.

36. Reinhardt D, Pesce E-R, Stieger P, Mandel T, Baltensperger K, Bennett M, Traas J, Friml J, Kuhlemeier C. Regulation of phyllotaxis by polar auxin transport. Nature. 2003;426:255–260. doi:10.1038/nature02081.

37. Reinhardt D, Frenz M, Mandel T, Kuhlemeier C. Microsurgical and laser ablation analysis of leaf positioning and dorsoventral patterning in tomato. Development. 2005;132:15–26. doi:10.1242/dev.01544.

38. Verwoerd TC, Dekker BMM, Hoekema A. A small-scale procedure for the rapid isolation of plant RNAs. Nucleic Acids Res. 1989;17:2362. doi:10.1093/nar/17.6.2362.

39. Nuwaysir EF, Huang W, Albert TJ, Singh J, Nuwaysir K, Pitas A, Richmond T, Gorski T, Berg JP, Ballin J, et al. Gene expression analysis using oligonucleotide arrays produced by maskless photolithography. Genome Res. 2002;12:1749–1755. doi:10.1101/gr.362402.

40. Irizarry RA, Hobbs B, Collin F, Beazer-Barclay YD, Antonellis KJ, Scherf U, Speed TP. Exploration, normalization, and summaries of high density oligonucleotide array probe level data. Biostatistics. 2003;4:249–264. doi:10.1093/biostatistics/4.2.249.

41. Garcion C, Metraux JP. FiRe and microarrays: a fast answer to burning questions. Trends Plant Sci. 2006;11:320–322. doi:10.1016/j.tplants.2006.05.009.

42. Dereeper A, Guignon V, Blanc G, Audic S, Buffet S, Chevenet F, Dufayard J-F, Guindon S, Lefort V, Lescot M, et al. Phylogeny.fr: robust phylogenetic analysis for the non-specialist. Nucleic Acids Res. 2008;36:W465–W9. doi:10.1093/nar/gkn180.

43. Long JA, Moan EI, Medford JI, Barton MK. A member of the KNOTTED class of homeodomain proteins encoded by the STM gene of Arabidopsis. Nature. 1996;379:66–69.

44. Kardailsky I, Shukla VK, Ahn JH, Dagenais N, Christensen SK, Nguyen JT, Chory J, Harrison MJ, Weigel D. Activation tagging of the floral inducer FT. Science. 1999;286:1962–1965.

45. Mandel MA, Gustafson-Brown C, Savidge B, Yanofsky MF. Molecular characterization of the Arabidopsis floral homeotic gene APETALA1. Nature. 1992;360:273–277. doi:10.1038/360273a0.

46. Bradley D, Ratcliffe O, Vincent C, Carpenter R, Coen E. Inflorescence commitment and architecture in Arabidopsis. Science. 1997;275:80–83.

47. Hartmann U, Hohmann S, Nettesheim K, Wisman E, Saedler H, Huijser P. Molecular cloning of SVP: a negative regulator of the floral transition in Arabidopsis. Plant J. 2000;21:351–360.

48. Golz JF, Keck EJ, Hudson A. Spontaneous mutations in KNOX genes give rise to a novel floral structure in Antirrhinum. Curr Biol. 2002;12:515–522.

49. Kieffer M, Stern Y, Cook H, Clerici E, Maulbetsch C, Laux T, Davies B. Analysis of the transcription factor WUSCHEL and its functional homologue in Antirrhinum reveals a potential mechanism for their roles in meristem maintenance. Plant Cell. 2006;18:560–573.

50. Huijser P, Klein J, Lonnig WE, Meijer H, Saedler H, Sommer H. Bracteomania, an inflorescence anomaly, is caused by the loss of function of the MADS-box gene SQUAMOSA in Antirrhinum majus. EMBO J. 1992;11:1239–1249.

51. Bradley D, Carpenter R, Copsey L, Vincent C, Rothstein S, Coen E. Control of inflorescence architecture in Antirrhinum. Nature. 1996;379:791–797.

52. Masiero S, Li MA, Will I, Hartmann U, Saedler H, Huijser P, Scharz-Sommer Z, Sommer H. INCOMPOSITA:aMADS-box gene controlling prophyll development and floral meristem identity in Antirrhinum. Development. 2004;131:5981–5990.

53. Stuurman J, Jäggi F, Kuhlemeier C. Shoot meristem maintenance is controlled by a GRAS-gene mediated signal from differentiating cells. Genes Dev. 2002;16:2213–2218.

54. Tsukamoto A, Hirai T, Chin DP, Mii M, Mizoguchi T, Mizuta D, Yoshida H, Olsen JE, Ezura H, Fukuda N. The FT-like gene PehFT in petunia responds to photoperiod and light quality but is not the main gene promoting light qualityassociated flowering. Plant Biotechnol J. 2016;33:297–307:297–307.

55. Molinero-Rosales N, Jamilena M, Zurita S, Gomez P, Capel J, Lozano R. FALSIFLORA, the tomato orthologue of FLORICAULA and LEAFY, controls flowering time and floral meristem identity. Plant J. 1999;20:685–693.

56. Janssen B-J, Williams A, Chen J-J, Mathern J, Hake S, Sinha N. Isolation and characterization of two knotted-like homeobox genes from tomato. Plant Mol. Biol. 1998;36:417–425.

57. Reinhardt D, Frenz M, Mandel T, Kuhlemeier C. Microsurgical and laser ablation analysis of interactions between the zones and layers of the tomato shoot apical meristern. Development. 2003;130:4073–4083.

58. Krieger U, Lippman ZB, Zamir D. The flowering gene SINGLE FLOWER TRUSS drives heterosis for yield in tomato. Nat Genet. 2010;42:459–U138.

59. Burko Y, Shleizer-Burko S, Yanai O, Shwartz I, Zelnik ID, Jacob-Hirsch J, Kela I, Eshed-Williams L, Ori N. A role for APETALA1/

FRUITFULL transcription factors in tomato leaf development. Plant Cell. 2013;25:2070–2083.

60. Pnueli L, Carmel-Goren L, Hareven D, Gutfinger T, Alvarez J, Ganal M, Zamir D, Lifschitz E. The SELF-PRUNING gene of tomato regulates vegetative to reproductive switching of sympodial meristems and is the ortholog of CEN and TFL1. Development. 1998;125:1979–1989.

61. Nakano T, Kato H, Shima Y, Ito Y. Apple SVP family MADS-Box proteins and the tomato pedicel abscission zone regulator JOINTLESS have similar molecular activities. Plant Cell Physiol. 2015;56:1097–1106.

62. Hofer J, Turner L, Hellens R, Ambrose M, Matthews P, Michael A, Ellis N. UNIFOLIATA regulates leaf and flower morphogenesis in pea. Curr Biol. 1997;7:581–587.

63. Taylor S, Hofer J, Murfet I. STAMINA PISTILLOIDA, the pea ortholog of FIM and UFO, is required for normal development of flowers, inflorescences, and leaves. Plant Cell. 2001;13:31–46.

64. Hofer J, Gourlay C, Michael A, Ellis THN. Expression of a class 1 knotted1-like homeobox gene is down-regulated in pea compound leaf primordia. Plant MolBiol. 2001;45:387–398.

65. Hecht V, Laurie RE, Vander Schoor JK, Ridge S, Knowles CL, Liew LC, Sussmilch FC, Murfet IC, Macknight RC,Weller Jl. The pea GIGAS gene is a FLOWERING LOCUS T homolog necessary for graft-transmissible specification of flowering but not for responsiveness to photoperiod. Plant Cell. 2011;23:147–161.

66. Taylor SA, Hofer JMI, Murfet IC, Sollinger JD, Singer SR, Knox MR, Ellis THN. PROLIFERATING INFLORESCENCE MERISTEM, a MADS-box gene that regulates floral meristem identity in pea. Plant Physiol. 2002;129:1150–1159.

67. Foucher F, Morin J, Courtiade J, Cadioux S, Ellis N, Banfield MJ, Rameau C. DETERMINATE and LATE FLOWERING are two TERMINAL FLOWER1/CENTRORADIALIS homologs that control two distinct phases of flowering initiation and development in pea. Plant Cell. 2003;15:2742–2754.